

Tunable Two-Dimensional Photonic Crystal Slab Exhibiting Broadband Sub-Wavelength Resolution

Qi Wu and Won Park

Department of Electrical and Computer Engineering, University of Colorado
Boulder, Colorado 80309-0425, USA
Tel: (303) 735-3601; Fax: (303) 492-2758; Email: won.park@colorado.edu

Abstract

We studied negative refraction and sub-wavelength imaging by two dimensional photonic crystal (PC) slabs, including both square lattice and triangular lattice PCs. The focusing properties of PC slabs, which are strongly dependent on frequency and PC lattice structure, were investigated by employing the finite-difference time-domain (FDTD) method and the plane wave expansion method. Building on the recently proposed mechanically tunable PC concept, we demonstrated that superlenses with sub-wavelength resolution are achievable over a wide range of frequencies by mechanically tuning the PC slabs.

Keywords: Photonic Crystal, Negative Refraction, Superlens, Sub-Wavelength Resolution, Tunability

1. Introduction

Recently there has been extensive research on materials that have a negative index of refraction.¹⁻⁷ Pendry has studied materials with both ϵ and μ negative and suggested that these materials can be used to fabricate a superlens whose resolution is not constrained by the diffraction limit.⁸ Negative refraction is achievable in optical regime by photonic crystal (PC). Light propagation in two-dimensional (2D) PC has been studied theoretically by Notomi and negative refraction at the interface of PC structure has been experimentally observed by Kosaka et al.^{9, 10} In addition, Luo et al. showed that the negative refraction in a square lattice PC can be utilized to make a superlens with which sub-wavelength imaging can be achieved.¹¹ Wang et al. used a triangular 2D PC with an effective isotropic refractive index $n = -1$ and demonstrated unrestricted superlensing.¹²

In this paper, we studied negative refraction and sub-wavelength imaging by 2D square and triangular PC slabs. Due to the strongly resonant nature of negative refraction, the focusing property of a negative index lens exhibits acute frequency dependence, thereby putting a severe restriction on the operating

frequency range. One possible solution to this problem can be found by using the flexible PC concept recently proposed by Park and Lee.¹³ This scheme uses mechanical stress to dynamically control the photonic band structure and dispersion surfaces, thereby offering a new opportunity to construct a widely tunable superlens. In this paper, we report a systematic study on the refractive properties of various PC structures and on the relationship between the structural parameters and focusing characteristics. We used the finite-difference time-domain (FDTD) method¹⁴ and the plane wave expansion method^{15, 16} to model various lattice structures and demonstrated that a flexible PC slab can be used as a tunable superlens over a broad range of frequency.

2. Results and Discussion

We first examined a 2D PC slab composed of a square lattice of air holes in silicon with a dielectric constant of $\epsilon = 12$. The PC is oriented in such a way that the interface is along the Γ -M direction. The radius of air holes is $r = 0.35a$ where “a” is the lattice constant. This structure has been shown to exhibit all angle negative refraction (AANR) for the transverse electric (TE, electric field in the plane) mode near the top of the first photonic band.¹¹ In this region, the equi-frequency surfaces (EFSs) become more convex as the frequency is increased. Therefore, we expect that the higher the frequency of the incident wave, the larger the refraction angle will be. This change will consequently affect the focusing properties of our PC slab. From a simple analysis based on geometrical optics, we expect that a point source with a higher frequency will generate an image located farther away from the slab.

In order to directly investigate how the focusing properties change with frequency, we performed point source imaging simulations using the FDTD method. The computational domain contained a PC slab of 30 x 5 unit cells sandwiched between air regions and was terminated with the perfectly matched layer boundary condition.¹⁷ We investigated the TE mode and

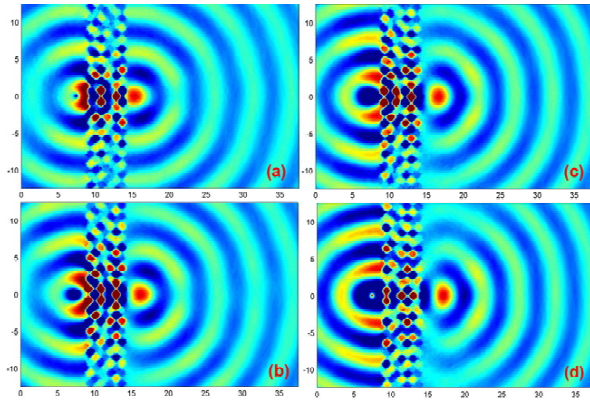


Fig. 1: H_z (magnetic field) fields of point sources and their images across a 2D square PC slab, at varying source frequencies as (a) 0.192, (b) 0.195, (c) 0.197 and (d) 0.200 (in unit of $2\pi c/a$). The location of the point sources is all the same: at a distance of $1.08a$ from the left edge of the slab.

the focusing properties by obtaining the magnetic field distribution. We placed a continuous-wave (cw) point source at a distance $1.08a$ from the surface of the PC slab and varied the frequency from $\omega = 0.192, 0.195, 0.197$ to 0.200 (in unit of $2\pi c/a$). As shown in Fig. 1, point images were found on the other side of the slab at distances of $1.13a, 1.83a, 2.25a$ and $2.67a$. This result clearly shows that the image moves away from the slab when the frequency of the source is increased, as predicted by the analysis based on the EFS. We also measured the lateral size (full width at half maximum) of the images and they were $0.33\lambda, 0.36\lambda, 0.42\lambda$ and 0.45λ respectively (λ is the source wavelength). All of the images exhibited sizes well below the source wavelength, clearly demonstrating the sub-wavelength resolution achievable in this frequency range.

However, the severe chromatic aberrations due to the rapidly changing of EFSs as a function of frequency imposes strict restrictions on the practical use of the negative index lens. This restriction, however, can be relieved by the recently proposed flexible PC concept in which photonic band structure is tuned by mechanical stress.¹³ Building on this new concept, we investigated the effect of mechanical stretching and compression of the square lattice structure along one of the Γ -M direction (vertical direction in our figures) while keeping the horizontal dimension unchanged.

In Fig. 2, we show two groups of FDTD simulations: one for perfectly square lattice and 2%, 5% stretched lattices (2% stretched lattice means the distance of two neighboring air holes along the stretching Γ -M direction is 2% longer than that in the perfectly square lattice) at a frequency of 0.190 (Fig. 2 a1 - a3); the other one for perfectly square lattice and 2%, 5% compressed lattices at a frequency of 0.205

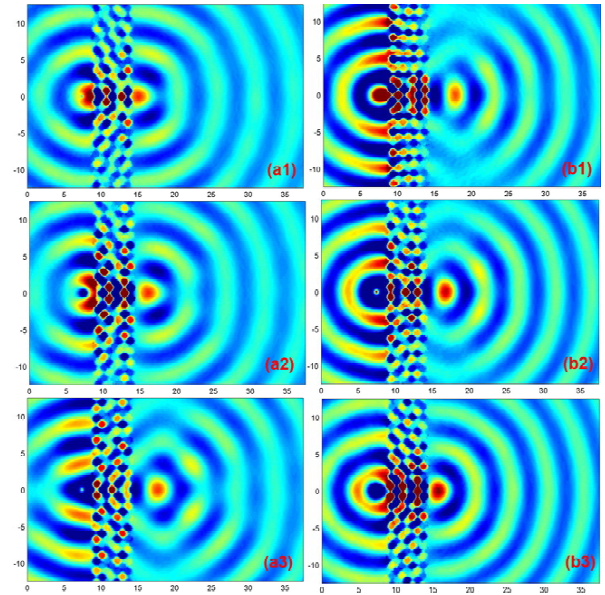


Fig. 2: H_z (magnetic field) fields of point sources and their images across a 2D square PC slab for varying the lattice structures (perfectly square lattices, stretched lattices and compressed lattices) at two frequencies 0.190 (a1-a3) and 0.205 (b1-b3). The positions of the sources are the same: at a distance of $1.08a_0$ from the left edge of the slab.

(Fig. 2 b1 - b3). At the frequency of 0.190 (in unit of $2\pi c/a_0$, a_0 is the lattice constant of the perfectly square lattice), the more we stretched the PC lattice, the farther the image moved away from the PC slabs. In the perfectly square lattice (a1), the image was at a distance of $0.79a_0$ from the right edge of the PC slab. In the 2% and 5% stretched lattices (a2 and a3), images were located at $1.83a_0$ and $3.50a_0$ from the slab, respectively. At the frequency of 0.205, on the other hand, the more we compressed the PC lattice, the shorter the image distance became. The image positions in these three cases (b1, b2 and b3) were: $3.29a_0, 2.46a_0$ and $1.62a_0$, respectively. These results clearly showed the possibility of engineering the focusing property with a relatively simple modification of the PC lattice. We also note that sub-wavelength resolution was achieved in all cases. The lateral sizes of the images in a1 - a3 were $0.35\lambda, 0.35\lambda$ and 0.38λ . In b1 - b3, they were $0.48\lambda, 0.43\lambda$ and 0.40λ , respectively.

Combining the effects of mechanically tuning the lattice structures and changing the source frequency, we arrive at the following conclusion: for each lattice structure and the frequency range we studied, increasing the frequency makes the image move away from the slab; however, at a fixed frequency, compressing the lattice pulls the image towards the slab while stretching it pushes the image away from the PC. Understanding these characteristics of the PC

slab enabled us to obtain lenses with the same focusing properties over a range of frequencies by mechanically tuning (stretching or compressing) the PC slabs. For example, we can compress the PC lattice and use it at a higher frequency. Because compressing the PC lattice and increasing frequency change the focusing property in the opposite way, compressing the lattice can compensate the effect of increasing frequency. Similarly, stretching the lattice makes the lens retains the same focusing characteristics at lower frequencies.

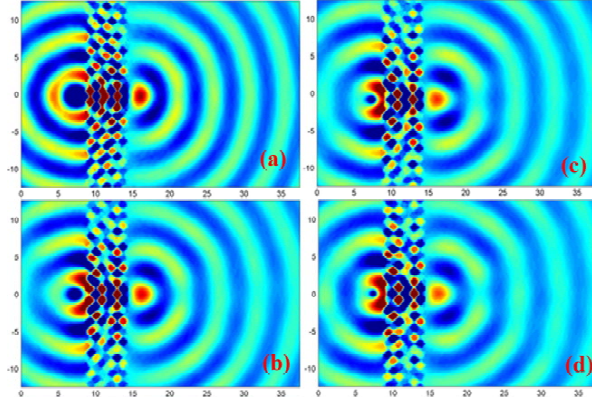


Fig. 3: H_z (magnetic field) fields of point sources and their images across a 2D square PC slab for varying both the lattice structure and frequency. They are 5% compressed lattice at $\omega = 0.207$ (a), perfectly square lattice at $\omega = 0.195$ (b), 2% stretched lattice at $\omega = 0.190$ (c) and 5% stretched lattice at $\omega = 0.185$ (d). The positions of the sources are also at a distance of $1.08a_0$ from the left edge of the slab. The images are all about $1.83a_0$ from the slabs.

To demonstrate this, FDTD simulations were performed as we changed both the lattice and the frequency. Fig. 3 shows several lattice structures which represent lenses with the same focusing characteristics at different frequencies. The perfectly square lattice slab was used for a frequency of 0.195 (Fig. 3(b)). At 0.190, we could use the PC lattice stretched by 2% along the Γ -M direction to get the same focusing property (Fig. 3(c)). And a lens working at the normalized frequency of 0.185 was achieved by stretching the perfectly square lattice by 5% (Fig. 3(d)). On the other hand, compressing the lattice by 5% makes it suitable for use at a frequency of 0.207 (Fig. 3(a)). All of these four lenses generated images located at a distance of $1.83a_0$ away from the slab. Again, sub-wavelength resolution was observed as we measured the lateral size of the images: (a) 0.40λ , (b) 0.36λ , (c) 0.35λ and (d) 0.35λ .

Various FDTD simulation results are combined in Fig. 4 to demonstrate how the focusing properties of the PC slabs change with respect to frequency and

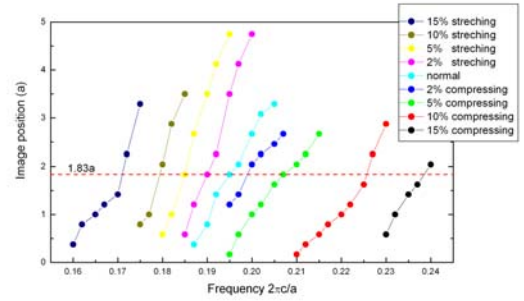


Fig. 4: Image positions varying with PC slabs of different lattice structure at a range of frequencies.

mechanical stress. The results are consistent with our preceding analysis. It can be seen clearly that the image distance increases as the frequency is increased and as the lattice is stretched. The data points on the red dash line are the four circumstances we showed in Fig. 3. We note that the focusing property can be varied continuously with the mechanical stress. Therefore, a lens exhibiting the same image distance of $1.83a_0$ for a frequency of 0.200, for example, can be made by compressing the perfectly square lattice slightly greater than 2%. We can also make a lens for a frequency of 0.205 by compressing the square lattice a little smaller than 5%. In principle, we are able to design lenses made of PC slab for a board range of frequency by mechanically tuning the slab. A desired focusing property is represented by a horizontal line in Fig. 4. Then, a proper lattice structure can be found by stretching or compressing the perfectly square lattice for any desired frequency within the range. In the case shown in Fig. 4, we could maintain the same focusing characteristics from 0.172 to 0.238 by mechanically stressing the PC lattice up to 10%. This represents a 32% tuning range with respect to the center frequency, i.e. $\Delta\omega/\omega_0 = 0.32$. We also note that finite element modeling showed flexible polymers such as PDMS can be deformed completely elastically for mechanical strain of up to 10%. The wide range of operating frequency achievable by the flexible PC lens will prove critical for practical applications of negative index lenses. Our theoretical study is the first attempt to quantify the relationship between mechanical stress on the PC lattice and change of frequency.

We also investigated a triangular lattice PC slab. The PC slab has air holes of radius $r = 0.4a$ in a dielectric material with $\epsilon = 12.96$. This structure has been shown to exhibit unrestricted sub-wavelength imaging for the transverse magnetic (TM) mode near the top of the second photonic band.¹²

We applied mechanical stress to the triangular lattice by stretching or compressing along the Γ -K direction (vertical direction in Fig. 5) and we studied

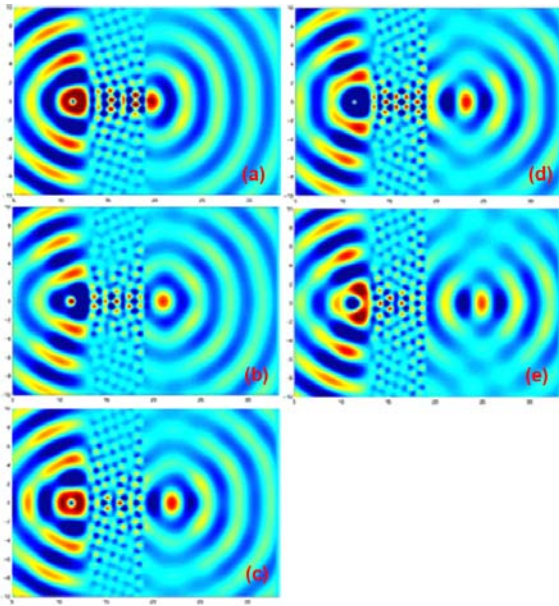


Fig. 5: E_z (electric field) fields of point sources and their images across a 2D triangular PC slab for varying the lattice structures at a frequency of 0.290. They are 5% compressed lattice (a), 2% compressed lattice (b), perfectly triangular lattice (c), 2% stretched lattice (d) and 5% stretched lattice (e). The positions of the sources are the same: at a distance of $2a_0$ from the left edge of the slab.

five lattice structures: 5% and 2% compressed lattices, 2% and 5% stretched lattices and perfectly triangular lattice. At a fixed frequency $f = 0.290$ (in unit of where a_0 is the lattice constant of the perfectly triangular lattice), those lattices showed the same trend as the square lattice did: the more we increase the vertical dimension of the PC lattice, the farther the image moves away from the PC slabs. As shown in Fig 5, the point sources are at a distance of $2a_0$ away from the slab. In the 5% and 2% compressed lattices (a and b), the images were at a distance of $0.40a_0$ and $1.83a_0$ from the right edge of the slab. With a perfectly triangular lattice (c), the image position is at $2.80a_0$. In the 2% and 5% stretched lattices (d and e), images were located at $3.97a_0$ and $5.73a_0$ from the slab. We also noted that sub-wavelength resolution was achieved in all cases. The lateral sizes of the images in a - e were 0.56λ , 0.50λ , 0.58λ , 0.62λ and 0.68λ , respectively. This result indicates that we can design a broadband superlens using a flexible triangular PC structure too. The difference in this case compared to the square lattice is that the EFS is nearly circular and thus isotropic negative refraction is expected.

3. Conclusion

In conclusion, we investigated the superlensing effect by 2D square and triangular PC slabs. We

showed that images with sub-wavelength resolution can be obtained over a wide range of frequency. However, the focusing properties are strongly dependent on the source frequency. Extending the recently proposed mechanically tunable PC concept,¹³ we studied the focusing properties of various PCs with different lattice structures. By conducting extensive numerical simulations, we obtained quantitative data on the achievable tunability and the required mechanical stress for the square and triangular PCs. The achievable tuning range for the square lattice PC was as large as 32% of the center frequency. This scheme provides a new means to design a widely tunable superlens based on a negative index PC slab, opening a door to practical applications of negative index lens.

4. References

- [1] V. G. Veselago, Sov. Phys. Usp. 10, 509 (1968).
- [2] J. B. Pendry, A. J. Holden, W. J. Stewart, and I. Youngs, Phys. Rev. Lett. 76, 4773 (1996).
- [3] J. B. Pendry, A. J. Holden, D. J. Robbins, and W. J. Stewart, IEEE Trans. Microwave Theory Tech. 47, 2075 (1999).
- [4] D. R. Smith, W. J. Padilla, D. C. View, S. C. Nemat-Nasser, and S. Schultz, Phys. Rev. Lett. 84, 4184 (2000).
- [5] D. R. Smith, S. Schultz, P. Markos, and C.M. Soukoulis, Phys. Rev. B 65, 195104 (2002).
- [6] R. A. Shelby, D. R. Smith, and S. Schultz, Science 292, 77 (2001).
- [7] M. Bayindir, K. Aydin, E. Ozbay, P. Markos, and C.M. Soukoulis, Appl. Phys. Lett. 81, 120 (2002).
- [8] J. B. Pendry, Phys. Rev. Lett. 85, 3966 (2000).
- [9] M. Notomi, Phys. Rev. B 62, 10 696 (2000).
- [10] H. Kosaka, T. Kawashima, A. Tomita, M. Notomi, T. Tamamura, T. Sato, and S. Kawakami, Phys. Rev. B 58, R10096 (1998).
- [11] C. Luo, S.G. Johnson, J. D. Joannopoulos, and J. B. Pendry, Phys. Rev. B 65, 201104 (2002).
- [12] X. Wang, Z. F. Ren and K. Kempa, Opt. Express 12, 2919 (2004).
- [13] W. Park and J.B. Lee, Appl. Phys. Lett. 85, 4845 (2004).
- [14] K. S. Yee, IEEE Trans. Antennas Propag. 14, 302 (1966).
- [15] J. D. Joannopoulos, R. D. Meade, and J. N. Winn, Photonic Crystals: Molding the Flow of Light (Princeton University Press, Princeton, 1995).
- [16] S. G. Johnson and J. D. Joannopoulos, Opt. Express 8, 173 (2001).
- [17] J. P. Berenger, J. Comput. Phys. 114, 185 (1994).